Deep Water Wave Measurements from Subsurface Buoys

Methods to Improve Data Quality by Correcting for Sensor Motion Bias

Jon D. Wood
Ocean Data Technologies, Inc.
Hyannis, MA 02601
jwood@oceandatatech.com

J. Anthony Schanzle
JAS Research, Inc.
Belmont, MA 02478
anthony.schanzle@gmail.com

Dr. Eugene A. Terray
Woods Hole Oceanographic Institution
Woods Hole, MA 02543
eterray@whoi.edu

Abstract- We describe various methods of correcting wave measurements obtained from upward-looking acoustic Doppler current profilers (ADCPs) mounted on subsurface buoys. Subsurface buoys are forced by both horizontal currents and surface waves, and so the resulting signals also include translational and rotational motions, which must be removed to maximize the accuracy of the results. We describe our most recent experience where estimates of buoy motion were obtained from an inertial motion unit (IMU) consisting of tri-axial accelerometers, rate gyros, and magnetometers. The platform motions were validated by comparing to independent motion estimates from a co-located downward-looking ADCP. Careful synchronization of the IMU and ADCP signals and rotating velocities into a fixed geographic reference frame allows us to subtract these motions from the upward-looking wave velocities, surface track, and pressures, and calculate wave height and directional spectra. Another critical adjustment was required for discretization errors arising from spatial changes in wave velocity between the ADCPs opposing beams, which becomes significant for higher-frequency waves. Since most of the translational movements of the buoy were in the horizontal plane (order ~50 cm/sec), with very little motion observed in the vertical plane (order ~ 5 cm/sec), corrections are more important for horizontal velocities than the vertical component. Wave height spectra derived from horizontal and vertical velocities, surface track, and pressure, were in remarkable agreement once corrections were applied. The effect of platform motion on the mean wave direction, which rely exclusively on the ratio of north and east velocities, also was small. We regard it good practice to correct for the full 3D velocity of the ADCP in order to maximize confidence in the resulting wave spectra. MEMS-based inertial sensors, of the kind used here, provide an excellent and low cost way of acquiring these data.

Keywords—waves, subsurface moorings, inertial sensing, ADCPs.

I. INTRODUCTION

Marine operations in deep-water regions, specifically oil and gas exploration activities, require an understanding of the mechanical loading imposed on floating platforms and vessels due to horizontal currents, winds, and ocean waves. Platform motions, particularly vertical heave and tilting oscillations, can have natural frequencies which reside at or near typical wave frequencies, causing potentially-problematic resonant responses. Accurately measuring the full wave spectrum in deep-water locations provides important benefits to offshore platform design and engineering efforts.

However, collecting quality wave data in deep water has proven a challenge. Traditional wave measurements techniques such as bottom-mounted, fixed sensor platforms are impractical in water depths greater than about 50 m. Since many projects take place in remote regions where surface-based instrumentation such as wave-rider-type buoys are at high risk of loss due to vessel and/or human interference, our preferred method of gathering these data has become mounting upward-looking acoustic Doppler current meters (ADCPs) within subsurface buoys. The lack of a surface presence eliminates associated risk of mooring loss or damage. The advantages of high probability of survival come however with a corresponding disadvantage, specifically, the contaminating effects of buoy motions to the resulting wave data.

The primary sensor used for our measurements is a Teledyne RD Instruments Workhorse 300 kHz acoustic Doppler current profiler, a four-beam Janus configuration with 20° beam angles. This ADCP is mounted in a subsurface buoy positioned nominally 20-30m below the surface. The buoy is constrained only by the mooring line, so free to oscillate laterally – and in a limited manner vertically - under force of steady horizontal currents and passing waves. To understand the underlying problem we consider the ideal case of a perfectly flat sea with zero waves, but with a steady horizontal current. A subsurface buoy in steady horizontal flows responds in two ways, one, a mean tilt in the downstream direction due to current-induced layover, and two, a low-frequency yawing motion due to vortex shedding off the buoy. In our experience, the mean tilts are order (0-

978-0-933957-43-5 ©2015 MTS

10°) and the yawing periods order (20-30 seconds). The combination of the mean tilt and yawing oscillations create 'wavy' signals in the pitch/roll, radial velocity, surface track, and pressure measurements, even with an ideal flat sea surface. These wavy signals would be the same as if the sensor were stationary in non-zero wave conditions. In simple terms, these buoy motions create false wave signals that will contaminate the data, leading to inaccuracies in the spectral distribution of wave energy. Further, if we now add also an oscillatory wave field to this case, such that the buoy moves in phase with passing waves while tilting and yawing, there is no way of distinguishing true wave motions from platform response. Removing the biasing effects of these motions is essential to maximizing accuracy of the resulting wave measurements.

Several projects have been completed, each project improving our ability to detect buoy motion and remove from the final wave height estimates. An early effort in the Makassar Strait (water depth 290m) collected more than a year of wave observations using just a single upward-looking ADCP with no motion corrections. The wave field was dominated by locally-generated, higher-frequency wind waves. Effects of buoy motion and bias introduced by the non-stationary wave measurement platform were assessed by analyzing ADCP tilt signals. The variance of pitch and roll signals appeared correlated more closely to horizontal current speeds than wave heights, suggesting buoy motions resulted primarily from variability of horizontal currents. Regarding data quality, wave height calculations using each of the ADCP's independent wave measurement methods agreed well for a majority of spectra. At lower frequencies, wave heights calculated from the velocity and pressure signals were consistent for most conditions, while surface track and velocity spectra were consistent generally at higher frequencies. Agreement between the three independent wave measurement techniques (velocity, pressure, and surface track) provided confidence the measurement approach was reasonable. However, variance was also detected at times in the swell wave band (~10-14 seconds), frequencies important for platform response design. Without an effective means of measuring buoy motion, questions were raised regarding the validity (or even existence) of the swell wave observations. Was the low-frequency energy real swell waves – a potential concern for operators in that region – or instead simply buoy motions?

Our next attempt was along the southern continental slope of Australia in approximately 1410 m water depth during the austral winter, collecting about 6 months of wave measurements from April to October. The buoy was positioned between 20-and-30 m below the surface. But some method of quantifying buoy motion was required for this project, so we mounted two (2) ADCPs in the upper buoy, one unit looking upward to the surface and the other looking downward into deeper water [1]. Both ADCPs were configured for wave burst sampling. The two ADCPs were fixed rigidly in the same buoy with the opposing acoustic beams aligned in the vertical, meaning beams 3 and 4 of both ADCPs pointed in the same directions, as did the opposing beams 1 and 2. The idea behind the up/down ADCP method assumed the downward-looking ADCP data measured wave orbital velocities in deep layers, about 100 m below the surface where, according to the dispersion theory, velocities would be largely attenuated, especially shorter-length waves. Hence, velocities at wave frequencies measured at distal bins were assumed a reasonable proxy estimate of buoy motion. These deep reference velocities were subtracted from the upward-looking ADCP measurements in the time domain. The resulting corrected velocities were used to calculate wave spectra. Wave measurements collected during this program showed significant wave heights ranged between 2 m to more than 10 m, with a maximum significant wave height of 10.6 m. Most of the wave energy was centered at sea swell frequencies (10 to 20 s); wind waves of shorter periods (5 to 10 s) were relatively less energetic. Analysis of the downward-looking velocity measurements in deep layers suggested the buoy was forced primarily by long-period swell and oscillated horizontally in phase with the wave orbital velocity but was constrained vertically by the mooring line [2].

Another subsurface mooring of the same design was deployed offshore of West Papua, Indonesia, northwestern Arafura Sea, in about 1400 m water depth, again using tandem upward- and downward-looking ADCPs in the upper buoy. However, for this project, and based on discussions after the Australia program, we also included a third device, an inertial motion unit (IMU), which was mounted also within the buoy well, bolted to the upward-looking ADCP near the center of buoyancy. The IMU was developed specifically to provide cost-efficient, independent measurements of buoy translational and angular motions; the IMU design specifications and performance evaluation was detailed in [3]. The IMU was programmed to burst-sample buoy motions simultaneous with ADCP wave bursts. Waves at this location were small and short, with most wavelengths less than the spread of the ADCP's beams. The buoy was subject to significant layover due to strong semi-diurnal tides, descending from its nominal depth of 27m to as deep as 94m at times. These strong currents induced a persistent tilt in the downstream direction and an oscillatory yawing due to vortex-shedding off the buoy, creating apparent velocities in upper (and deeper) bins with periods roughly 15-20 s.

II. Gulf of Guinea Deployment

Our most recent deployment was for 60-days in the Gulf of Guinea, off the coast of West Africa, in 92 m water depth very close to the continental shelf break where the slope descends steeply offshore. We will draw upon this data set to demonstrate the data processing techniques.

A. Deployment and Data Description

We mounted upward- and downward-facing 300 kHz TRDI "Workhorse" ADCPs at the top and bottom of a 49" syntactic foam sphere, which also housed battery cases and an inertial motion unit (IMU) which was located near the center of buoyancy. Together the two ADCPs provided current profiles over the full water column. The float was deployed at a target depth of 21 m. Mean currents at this location were eastward, parallel to the shelf break, with occasional brief reversals to the west. Currents at the buoy depth averaged 0.30 m/s, with a peak speed 1.1 m/s. Speeds were less than 0.50 m/s about 90% of the time. Consequently, very little buoy layover was observed, and the float remained at the target depth most of the time. The highest significant wave height measured during the deployment was 2.6 m with a peak period of around 12.5 s, and the average significant wave height over the deployment was 1.24 m. The waves were predominantly from the southwest, or approximately cross-shelf at this location. The wave height spectrum generally showed a dominant peak at lower frequencies due to swell, and a second one at higher frequency associated with wind-generated waves. We also observed yawing and tilting motions with periods in the range 25-28 s which we attribute to current-induced vortex-shedding from the sphere [3].

The upward ADCP used the TRDI 'packets' mode and sampled five 1-m range cells at a 2 Hz rate. Data were collected in 20 minute 'bursts' every three hours. The location of the range cells was auto-selected at the start of each burst based on the mean depth of the instrument. Two were close to the ADCP and another three close to the surface. Velocities in each range cell were recorded in radial (beam) coordinates. In addition, the instrument recorded pressure, heading, pitch and roll, and the vertical distance to the surface (*i.e.* 'surface-track') along each beam. The downward-looking ADCP collected data at the same sample rate and burst schedule, but with a 4 m range cell. Due to the water depth we did not attempt to record surface-track data.

The IMU was a Microstrain (Lord Corp.) 3DM-GX3-25 attitude-heading-reference sensor (AHRS). The data from this device were logged using a CF-2 single-board computer (Persistor Instruments). The logger and power supply were developed by us and are described in [3]. The 3DM combines tri-axial accelerometers, rate-gyros, and magnetometers, a temperature sensor, and an on-board processor to estimate the sensor orientation (attitude and heading) in real-time. We additionally recorded the calibrated accelerations, angular rates and magnetic field components for our own later processing. All of the 3DM data were logged at 40 Hz, nominally on the same burst schedule as the ADCPs (the 3DM's internal processing rate is 1 kHz which enables correction of the internally-computed orientation for coning motions). The three instruments were rigidly mounted with respect to one another, and we took some care to align them as closely as possible. Note, however, that the exact alignment is not essential because the mean orientation recorded by each instrument can be used to establish the alignment if the accelerometer and magnetometer biases are known and are stable (which usually is the case).

B. IMU Data Processing

The drift rate and precision of the MEMS-based sensors used in the 3DM prevents it from being used to estimate position. But because wave-induced motion is oscillatory, we were optimistic that the accelerations could be integrated once to estimate velocities in the wave band. That this can be done successfully is not obvious because the integration must be performed in a non-moving reference frame, and hence the measured accelerations must first be transformed to fixed coordinates using the estimated IMU attitude and heading. Estimating orientation presents a similar problem because rate gyros measure angular rate, and hence must be integrated to compute angle. This is accomplished internally within the 3DM using a complementary filter (CF) to estimate orientation from the inertial measurements by combining the attitude and heading computed from the low-passed accelerometer and magnetometer outputs with the three integrated high-pass filtered angular rates. The CF is constructed from low-pass and high-pass filters having the same 3dB frequency, with the constraint that $|L|^2 + |H|^2 = 1$, where $L(\omega)$ and $H(\omega)$ denote the two transfer functions. Consequently, at sufficiently high frequencies the orientation is determined entirely by the integrated angular rates, whereas for frequencies approaching zero the attitude is computed from the accelerometer output. Although the CF approach is not based on an optimality criterion, it is attractive because of its low implementation and computational overhead. However, it relies critically on the assumption that the translational acceleration is negligible at frequencies well-below the 3dB cutoff. As a result, the performance of the technique depends on the spectral characteristics of the data. The CF internal to the 3DM-GX3-25 uses single-pole filters. Since the roll-off of these filters is only 6dB/octave, some of the accelerometer output 'leaks' into the estimate of pitch and roll in the wave band, and similarly, the estimate of attitude at low frequencies is biased by leakage of the integrated rate-gyro output. Since the expected frequency of the dominant waves was expected to be of order 0.1 Hz, we set the 3dB "crossover" frequency to approximately 1/126 Hz.

As a check on the performance of the internal 3DM CF, we also post-processed the inertial measurements using a CF constructed from 4^{th} order Butterworth high-pass and low-pass filters having a 3dB frequency of 1/60 Hz. These were applied to the data in both the forward and reverse directions in order to remove the nonlinear phase shift. As a result, the effective out-of-band attenuation of the filters was 48 dB/octave. The standard deviation of the differences in the pitch, roll and heading Euler angles obtained using this CF to those computed internally in the 3DM were 0.20, 0.16 and 0.42 degrees, respectively. Since the agreement is quite good, for these data the internal CF was adequate and leakage due to the low filter order did not significantly affect the estimated orientation.

C. Motion Correction

Since the motion correction procedure is performed in the time domain it is critical to synchronize all of the data sets as closely as possible. The IMU and two ADCPs had independent clocks. Although we synchronized them at the start of the deployment, they drifted over time at different

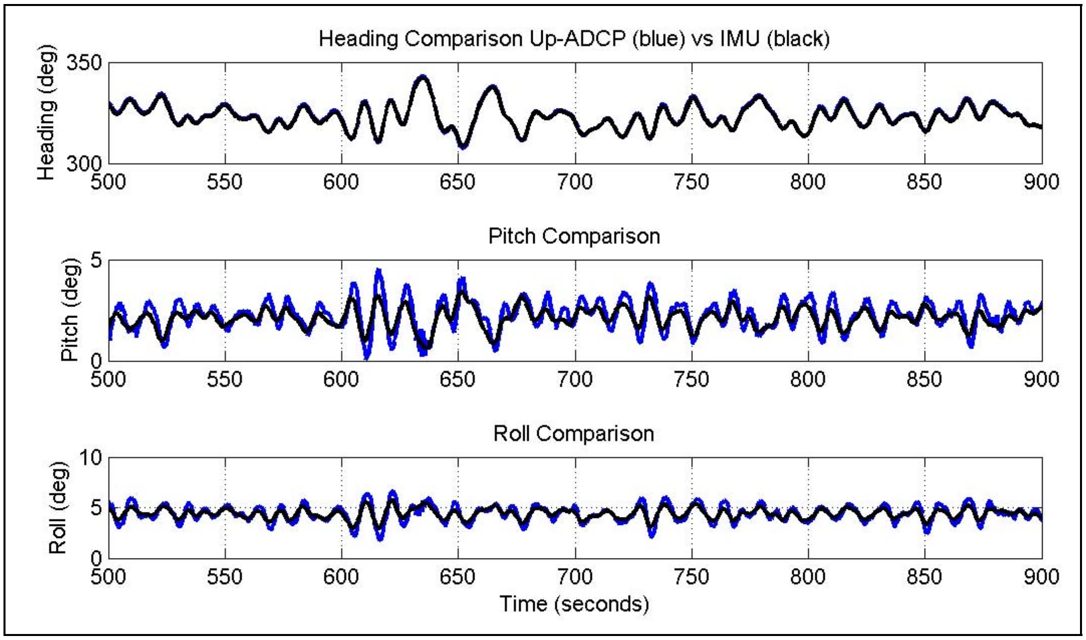

Figure 1: Comparison of the IMU-generated heading, pitch, and roll signals (black) versus those recorded by the up-ADCP (blue) for a short subsection of a burst. Unlike the ADCP, the IMU attitude signals are less noisy and are not biased by lateral accelerations.

rates (for example, at the end of the 60-day deployment the two ADCP clocks differed by roughly 2 minutes). We re-synchronized the three instruments for each burst by comparing a common signal – in this case the heading which showed a large, narrowband oscillation with a period of around 25 s. For each burst, we found the lag of the maximum cross-correlation between sensor pairs. We then fit a straight line using least-squares to the collection of lags for that pair and used the estimated drifts to align the three time series in each burst.

The velocities along opposing beams of the upward-looking ADCP were first combined (in the same way as is usually done to estimate currents) to give velocities in TRDI-defined “ship” coordinates (*i.e*. starboard, forward and mast) [4]. Because the wave velocities varied spatially between the beams, this procedure has errors that depend on the product of the wavenumber and the beam separation. We call this “discretization error” and discuss it in the next section. The velocities were then rotated sample-by-sample into a fixed (earth-referenced tangent plane) coordinate system. However, since the liquid-level tilt sensors in the ADCP are affected by lateral accelerations (which are indistinguishable from tilts), we chose instead to use the pitch and roll signals from the IMU for these rotations (resampled to the ADCP sample rate). Figure 1 shows the comparison of the IMU heading, pitch, and roll signals to those recorded by the upward-facing ADCP. Note that the IMU signals are less noisy, and do not have the overshoot common to the ADCP signals.

The motion of the subsurface float was estimated in two ways: directly from the downward-pointing ADCP, and by integrating the IMU accelerations. We discuss the ADCP processing first. The measured velocity at -76 m depth was used to estimate the float motion. As for the case of the up-ADCP, the four along-beam velocities were first combined into starboard-forward-mast components, which were then rotated into earth coordinates using the IMU orientation. Since the float motion is a spatially-uniform apparent velocity there is no discretization error arising from the spatial separation of the beams. Note, however, that the use of the velocity at depth as a surrogate for the float velocity rests on the assumption that any residual wave velocities at the reference bin are negligible.

The second method of estimating the float velocity is based on the IMU measurements. We first rotated the measured acceleration into earth coordinates using the IMU Euler angles. The leveled accelerations were then integrated using a trapezoidal rule to give earth-referenced velocities. These were then bandpass filtered with a 3dB passband of 0.02 – 1 Hz. The resulting IMU-based estimates of the east and north float velocities are compared in Figure 2 to the corresponding velocity components measured at -76 m by the downward- looking ADCP. The agreement is quite good. The standard deviation of the north velocity estimated by both devices is approximately 20 cm/s, whereas the standard deviation of the difference between the two estimates is 6.4 cm/s. Linear wave theory for intermediate depth water applied *a posteriori* to the height spectrum gives an estimate of 5 cm/s for the rms horizontal wave velocity at -72 m depth, so that much (but not all) of the difference can be explained by the residual wave orbital velocities at the reference depth. Although in previous deployments employing tandem ADCPs we had used a deeper reference cell, the relatively shallow water column prevented that here.

Once the velocities were synchronized and rotated into a fixed reference frame, the float velocity was subtracted from the up-ADCP. For the surface track and pressure time series, the buoy vertical heave was calculated and subtracted.

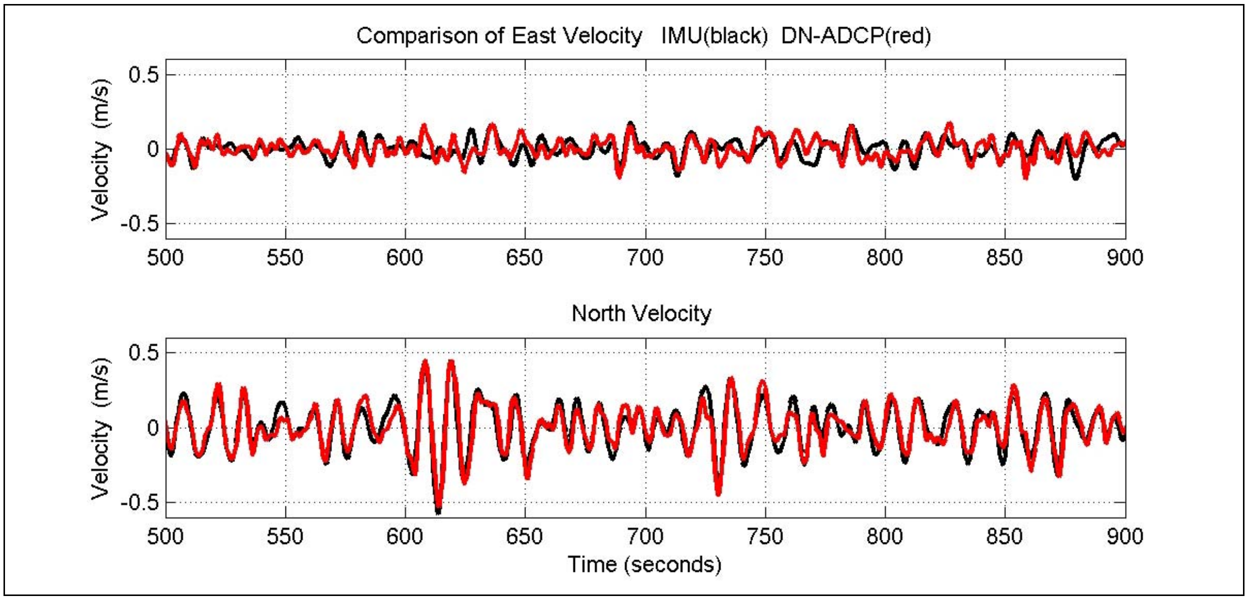

Figure 2: Comparison of the earth-referenced sensor motion velocities. The red curves depict the downward-looking ADCP velocities in the deep reference bin at -72m. The black curves show velocities determined by the IMU.

D. Bias Due to Discretization Error

Horizontal and vertical wave velocities are estimated by differencing and adding velocities measured along opposing beams of the upward-facing ADCP. Whereas this procedure is exact for velocities such as currents that (by conventional assumption) do not vary spatially across the aperture of the beams, in the case of waves, whose velocities vary spatially, this procedure is subject to a "discretization error". The relative error in the spectrum of the horizontal velocities due to this can be large.

The Fourier amplitudes in the frequency-domain of the "horizontal" and "vertical" velocities obtained from opposing beams along the starboard axis are:

$$\hat{U}_s(\omega) = \omega F \int_{-\pi}^{+\pi} d\theta \hat{\eta}(\omega,\theta) \left[\cos\theta \cos(k\Delta\cos\theta) + R\,\mathrm{ctn}\beta \sin(k\Delta\cos\theta) \right]$$

$$\hat{W}_s(\omega) = i\omega F \int_{-\pi}^{+\pi} d\theta \hat{\eta}(\omega,\theta) \left[\mathrm{R}\cos(k\Delta\cos\theta) - \tan\beta\cos\theta\sin(k\Delta\cos\theta) \right]$$

where $\hat{\eta}(\omega,\theta)$ denotes the Fourier amplitude of the surface displacement as a function of frequency and direction, 2Δ is the lateral separation of the range cells, the vertical structure functions for the horizontal and vertical velocity

$$F(kz) = \cosh[\mathrm{k}(z+D)]/\sinh(kD)$$

$$F'(kz) = \sinh[k(z+D)]/\sinh(kD)$$

$$R = F'/F = \tanh[k(z+D)]$$

(here $z < 0$ is the depth of the range cell below the mean surface, and D denotes the water depth) , and β (here 20°) is the beam angle (so that $\tan\beta \sim 0.364$ and $\mathrm{ctn}\beta \sim 2.75$). Note that for range cells close to the surface and deep water (*i.e.* $-z << D$ and $kd >> 1$), then $R \to 1$.

Expressions for the analogous forward-beam quantities can be obtained from the starboard velocities by replacing $\theta \to \theta - \pi/2$. The trigonometric factors appearing in the integrals can be expanded in terms of the directional harmonics $\exp(in\theta)$ with coefficients $\Gamma_n(\varepsilon)$ where $\varepsilon = k\Delta$. To leading order $\Gamma_n \sim (\varepsilon/2)^n/(n-2)!$. It turns out to result in more compact expressions to work with the linear combinations $\hat{U} = \hat{U}_s + i\hat{U}_f$ and $\hat{W} = (\hat{W}_s + \hat{W}_f)/2$.

We define the bias in the non-directional wave height spectrum estimated from $\hat{U}$ and $\hat{W}$ as

$$B_U = \left[S_U / (\omega F)^2 \right] \Big/ S_\eta$$

$$B_W = \left[S_W / (\omega F')^2 \right] \Big/ S_\eta$$

where $S_\eta(\omega)$ denotes the true wave height spectrum. Using the directional expansions of $\hat{U}$ and $\hat{W}$ described above we can similarly expand B_U and B_W as

$$B_U = \beta_0 - \beta_4 \langle \cos 4\theta \rangle + O(\varepsilon^6) \langle \cos 8\theta \rangle + \ldots$$

$$B_W = \alpha_0 - \alpha_4 \langle \cos 4\theta \rangle + O(\varepsilon^6) \langle \cos 8\theta \rangle + \ldots$$

where $\langle \ldots \rangle$ denotes an average over the frequency-direction spectrum, $D(\omega,\theta)$, normalized so that $|\langle \cos n\theta \rangle| \le 1$. Explicit expressions for the coefficients β_n and α_n as functions of ε are straightforward to work out. The first two coefficients for both the U and W height spectrum biases are given in the following table for the case of

Table I: Discretization Error as a Function of Frequency

f (Hz)	0.001	0.080	0.120	0.140	0.160	0.180	0.200
$\varepsilon = k\Delta$	0.001	0.141	0.313	0.426	0.557	0.704	0.870
β_0	1.01	1.90	3.29	4.32	5.56	6.97	8.44
β_4 / β_0 (%)	0.000	0.405	1.72	2.98	4.79	7.33	10.8
α_0	1.000	0.940	0.845	0.773	0.683	0.577	0.457
α_4 / α_0 (%)	0.00	0.00	0.059	0.168	0.424	1.01	2.23

a range cell at z = -10 m in 95 m water depth located Z = 15 m above the ADCP, so that (for a beam angle of 20°), Δ = 5.4 m.

From Table I we see that over the range $0 \le \varepsilon \le 0.9$ the 4θ harmonic is negligible for the W-bias and is at most roughly a 10% correction to the leading order U-bias. While $\langle \cos 4\theta \rangle$ is not known directly, it can be estimated from (for example) the maximum entropy estimate of the frequency-direction spectrum.

The mean wave direction can be estimated in the usual way for "triplet data" from the quadrature spectra of U_f and W and U_s and W which provide, respectively, estimates of $\langle \cos\theta \rangle$ and $\langle \sin\theta \rangle$. However, as above, these are biased by discretization error. Unlike the autospectra, however, the leading term in the bias is $O(\varepsilon^2)$. A short calculation shows that the estimate of the mean direction, $\hat{\theta}$, is

$$\hat{\theta}(\omega) = \theta(\omega) + \Lambda(k\Delta)\frac{\langle \cos\theta \rangle \langle \sin 3\theta \rangle + \langle \sin\theta \rangle \langle \cos 3\theta \rangle}{\langle \sin\theta \rangle^2 + \langle \cos\theta \rangle^2}$$

where θ denotes the true mean direction (at each frequency), and Λ ($k\Delta$) ~ O (ε^2) is a known function of ε. Note that unlike the autospectra, the leading term in the expression for the bias in direction is of order ε^2. As with the autospectra, the various trigonometric expectations are not known *a priori*, but could be estimated to leading order from the frequency-direction spectrum.

E. Estimates of Wave Height and Direction

One of the strengths of using an ADCP to measure waves is that it provides four redundant estimates of the wave height spectrum – to wit, from pressure, surface-track, and the horizontal and vertical wave velocities. Consistency of these over their domains of validity in frequency provides some confidence that a reliable estimate has been obtained. This paper has been primarily concerned with using the velocity spectra to estimate wave height by correcting the measured velocities for platform motion and discretization error (DE). Once these corrections have been made, we estimate the wave height spectrum by applying linear theory transfer functions for intermediate water depth to the horizontal and vertical velocity spectra as

$$S_{\eta U} = S_U / (\omega F)^2 \text{ and } S_{\eta W} = S_W / (\omega F')^2$$

To examine the importance of each correction more fully, we consider the following four cases:

1. Correction for both motion and (DE)
2. Correction for motion only, no DE adjustment
3. Correction for DE only, no motion adjustment
4. No correction for either motion or DE

The results for these four cases, applied to the horizontal and vertical velocity spectra, are shown in Figure 3. The left-hand plot represents the wave height spectra derived from horizontal velocities. The black line shows the fully-corrected case, with adjustments for both platform motion and discretization errors. However, the non-fully corrected cases have radically different spectral shapes. If only applying motion correction and ignoring the discretization error, then the spectrum is much too large both at the peak and at higher frequencies, over-predicting the true wave height. If only discretization effects are adjusted, but motion effects ignored, then the resulting spectrum is much too small, especially under the peak, and under-predicts the true wave height. And if neither corrections are made, the resulting spectrum bears no resemblance to the true wave height spectrum, leading to gross errors in both wave height and peak period. This suggests to us that adjusting the up-ADCP horizontal velocities for motion as well as discretization bias is an important consideration to achieve accurate results, and both appear to be of roughly equal importance

We note that neither the motion nor DE correction appears important in this deployment for the vertical velocity spectrum. This is consistent with the DE values shown in Table I, and the fact that a taut mooring in shallow water constrains vertical motion. Accordingly, buoy vertical velocities were quite small, of order a few cm/sec, and any corrections made for these small motions will have a corresponding small effect on the results. It is also encouraging that the observed attitude variability of ~O(5°) in pitch and roll did not have a significant effect on the vertical height spectrum. In this case at least, these results suggest wave heights derived from vertical velocities can be used 'as

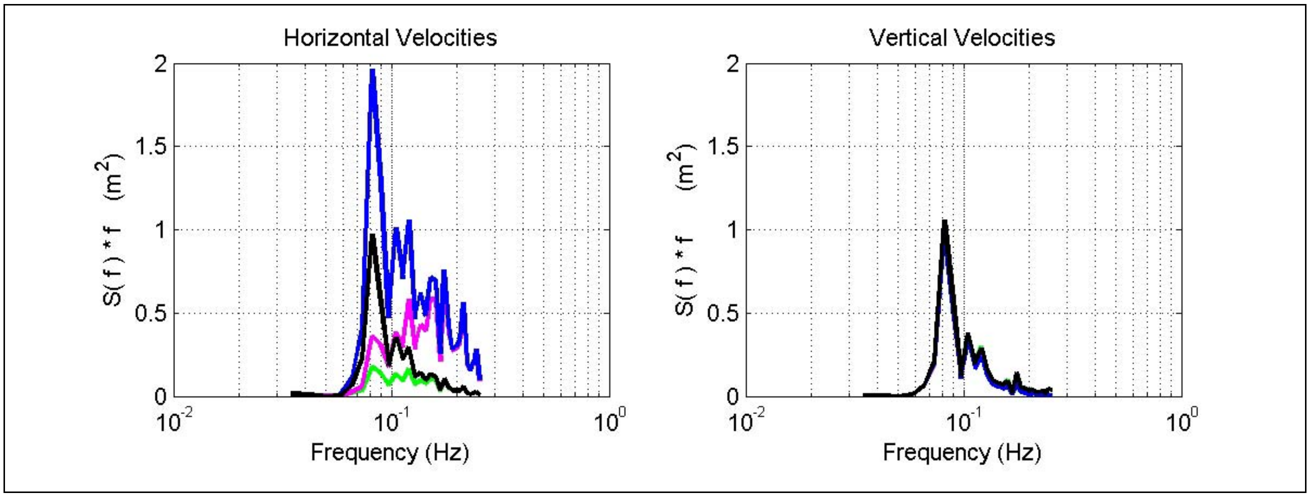

Figure 3: Comparison various combinations of motion and discretization error (DE) applied to the horizontal and vertical velocity spectra (in the earth frame) to estimate the non-directional wave height spectrum. The black lines represent case 1 (fully corrected results – both motion corrections and DE adjustments were made). The blue line represents case 2 -only motion corrections, while the green line represents case 3 -only DE corrections. The magenta lines represent case 4 - uncorrected results, with no motion or DE adjustments applied.

is' directly from the up-ADCP velocities without bothering to correct for platform motion. Of course, this presumes the mooring system to be sufficiently taut, which may not always be the case. For example, during our Australia project [2], we calculated vertical heave to be +/-3m for an estimated 7.6m wave height, and so in that circumstance using vertical velocity without correction may have introduced errors. Compensating heaving motion also is necessary for measurements from approximately neutrally-buoyant, unconstrained platforms, such as the AUV described in [5].

The best estimate of the wave height spectrum from each measured quantity (*i.e.* horizontal and vertical velocities, surface-track and pressure) is displayed in Figure 4, and show excellent agreement. The significant wave height was estimated from each spectrum by integrating over the respective frequency bands shown in Figures 3. The results are summarized in Table II (note that DE corrections are not relevant for pressure and surface-track spectra).

Table II: Significant Wave Height Estimates

Significant wave height (m)	Fully Corrected	No Motion No DE	Yes Motion No DE	No Motion Yes DE
Horizontal Velocity	2.22	2.60	3.76	1.33
Vertical Velocity	2.17	2.03	2.03	2.18
Surface-Track	N/A	2.32	2.32	N/A
Pressure	N/A	2.02	2.00	N/A

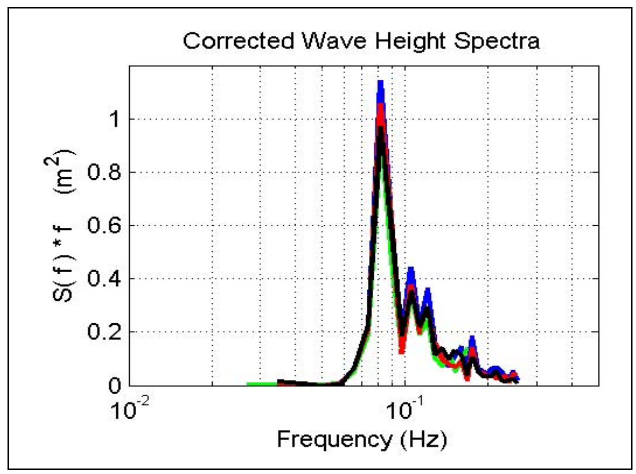

Figure 4: Best estimate of the non-directional wave height spectrum from the horizontal (black line) and vertical (red) velocities, surface-track (blue) and pressure (green) after applying motion and DE corrections.

The mean wave direction as a function of frequency was determined from the motion-corrected and uncorrected horizontal and vertical velocities, as discussed in Section C, but neglecting discretization error. The result is displayed in Figure 5. This figure shows that the mean wave direction is relatively insensitive to horizontal motions. However, this insensitivity may be a fortunate consequence of the wave direction in this particular circumstance. Since wave directions are to the north, with little-to-no easterly component, any change in the amplitude of the wave velocities due to motions – even a scaling of one-half say - will have little effect on the direction computation since the east component would remain proportionally small. We are unsure if the apparent insensitivity of wave directions to platform motions would remain if the waves were from a different direction where east and north velocity components were roughly similar. This is an issue for further study.

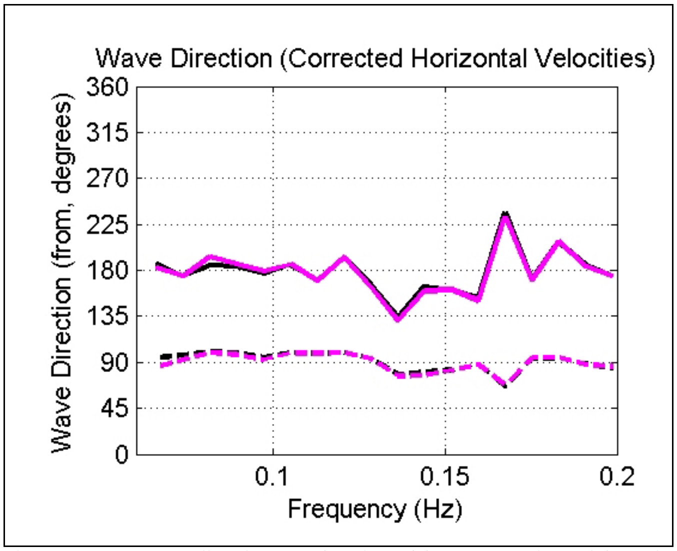

Figure 5. Mean wave direction as a function of frequency estimated from the quadrature spectra between the north and vertical velocity, and the east and vertical velocity. The coherence (%) between the north and vertical velocity components is shown as the dashed line. The black and magenta traces refer to the motion-corrected and uncorrected cases, respectively.

III. CONCLUSIONS

This paper continues our long-term effort to measure the heights and directional characteristics of ocean waves using moored subsurface ADCPs [1-3]. It extends recent work [3] that considered the effect of current-induced mooring motion on attitude measurements to include the effects of wave-forcing. In our previous experiments we deployed both upward- and downward-facing ADCPs and used the measured velocities at the deepest ranges as a proxy for the translational motion of the float. In addition to requiring a second ADCP, and its associated expense, this approach is sensitive to residual wave orbital velocities at the reference depth. This can be a problem in the presence of long ocean waves because their velocities penetrate deep into the water column.

Consequently we have investigated the use of an inexpensive, industrial-grade, attitude-heading-reference sensor (AHRS) to estimate the translational velocity of the float, as well as its orientation. The work presented here quantifies the performance of this class of devices and shows that they can be used in place of the down-ADCP for this purpose.

A second difficulty that restricts the application of this method is the fact that the lateral separation, 2Δ, between corresponding range cells in opposed upward-pointing beams increases with distance from the ADCP. Hence the range cells closest to the surface, which have the highest signal-to-noise ratio, are most strongly affected by discretization error (DE) due to the separation. We have shown that the DE in the estimate of the vertical wave velocity is smaller than the corresponding DE affecting the horizontal velocity estimate, and have presented a correction scheme for both spectra that is valid out to moderate values of $\varepsilon = k\Delta$. This analysis also shows that the leading DE term in the estimate of the mean wave direction is $O(\varepsilon^2)$. We remark that these results also extend the range of depths over which bottom-mounted ADCPs can be used to measure waves.

Lastly, we have shown that also correcting for the float motion is necessary in order to estimate the height spectrum with good fidelity. Although in the case of the data considered here there was no need for vertical motion correction because the float was constrained in that direction, there are deployment scenarios where the vertical motion is not insignificant [1,5], and we regard it as good practice to measure the full 3D velocity of the ADCP. MEMS-based inertial sensors, of the kind used here, provide an excellent and low cost way of acquiring these data.

REFERENCES

[1] Wood, J.D.; Terray, E.; Strong, B.; Singh, B. (2005).Measurement of deepwater ocean waves from a subsurface mooring. Oceans 2005 – Europe, pp. 166-171, Vol. 1, DOI: 10.1109/OCEANSE.2005.1511703

[2] Wood, J.D.; Terray, E.A. (2006). A mooring design for measurement of deep Water ocean waves. Oceans 2006 - Boston, pp. 1-6, DOI: 10.1109/OCEANS.2006.307064

[3] Schanzle, J.A.; Wood, J.D.; Terray, E.A. (2014). The use of low-cost inertial sensors to improve deep water wave and current measurements from subsurface moorings. Oceans 2014 - St. John's, pp. 1-6, DOI:10.1109/OCEANS.2014.7003228

[4] Teledyne RD Instruments Manual (2008). ADCP Coordinate transformation. TRDI Part number 951-6079-00.

[5] Haven, S.; Terray, E.A. (2015). Surface wave measurements from an autonomous underwater vehicle.IEEE/OES EleventhCurrent, Waves and Turbulence Measurement (CWTM), pp. 1-7, DOI: 10.1109/CWTM.2015.7098106